LOST IN SPACE: OPTIMAL TRIANGULATION FOR CELESTIAL LOCALIZATION

Sébastien Henry[1] and John A. Christian[1*]; [1] Georgia Institute of Technology, Atlanta, GA 30332.
[*]john.a.christian@gatech.edu

Abstract. *Optical measurements are a key part of modern interplanetary navigation. The statistically optimal Linear Optimal Sine Triangulation (LOST) algorithm is applied to the context of celestial navigation. In addition to optimal triangulation methods, celestial navigation requires the consideration or target ephemeris errors, light aberration, and light time-of-flight. In most cases, only light aberration and light time-of-flight change the expected direction of the measured line-of-sight (LOS). These effects are found to be non-negligible at typical observer velocities (for light aberration) and planet velocities (for light time-of-flight). The effects of the position uncertainty of planets are only important when the observer is close to them. The LOST framework provides a mechanism to conveniently consider all of these effects.*

Introduction. There has been much interest in recent years on navigation by celestial triangulation.[1–5] A review of the literature and practical application will reveal that two things are essential for such celestial triangulation schemes to be successful. First, the use of statistically optimal triangulation algorithms is required to produce the best-possible spacecraft localization from the available measurements. Second, we must consider a variety of real-world effects that are often neglected for generic (non-celestial) triangulation problems. This work discusses the specific effects of (1) planetary ephemeris and sensor attitude errors, (2) aberration of light, and (3) light time-of-flight. We note that a significant percentage of the contemporary celestial triangulation literature does not handle these effects correctly.

Overview of Celestial Triangulation. Consider the case of a spacecraft in a heliocentric orbit with position $\boldsymbol{r} \in \mathbb{R}^3$. Suppose this spacecraft is equipped with one or more optical sensor(s) that view(s) at least two ($n \geq 2$) celestial bodies that were located at heliocentric positions $\{\boldsymbol{p}_i\}_1^n \in \mathbb{R}^3$ when the observed photons were reflected by the body. If the observed celestial bodies are distant then they appear as an unresolved object in the image produced by the optical sensors (e.g., cameras, telescopes). Thus, since the observed body is unresolved, the sensors produce only line-of-sight (LOS) direction from the spacecraft to the observed body. We denote these LOS directions as $\{\boldsymbol{\ell}_i\}_1^n$,

$$\boldsymbol{\ell}_i \propto \boldsymbol{p}_i - \boldsymbol{r} \qquad (1)$$

where $\boldsymbol{\ell}_i \in \mathbb{P}^2$ and is a 3×1 vector of ambiguous scale. The celestial triangulation scenario described here is illustrated in Fig. 1.

Assuming the optical sensor is a camera or telescope that forms an image by perspective projection, we can express the vectors from Eq. (1) in the camera frame and directly write the pinhole camera model as

$$\begin{bmatrix} x_i \\ y_i \\ 1 \end{bmatrix} = \bar{\boldsymbol{x}}_i \propto \boldsymbol{\ell}_i \propto \boldsymbol{p}_i - \boldsymbol{r} \qquad (2)$$

where the two-dimensional coordinates $[x_i, y_i]$ describe the projection of the LOS $\boldsymbol{\ell}_i$ onto the image plane (i.e., where $\boldsymbol{\ell}_i$ pierces the $z = 1$ plane of the camera frame). The conversion from the image plane to pixel coordinates $[u_i, v_i]$ may be achieved with an affine transformation

$$\begin{bmatrix} u_i \\ v_i \\ 1 \end{bmatrix} = \bar{\boldsymbol{u}}_i = \boldsymbol{K} \bar{\boldsymbol{x}}_i \qquad (3)$$

where $\boldsymbol{K}$ is the camera calibration matrix. Further details on LOS measurements, camera models, and the camera calibration matrix may be found in Refs. 5 and 6.

Substitution of Eq. (3) into Eq. (2) allows us to take the measured pixel coordinates of an unresolved celestial body and construct the corresponding image plane coordinate or LOS direction in the camera frame:

$$\boldsymbol{\ell}_i \propto \bar{\boldsymbol{x}}_i = \boldsymbol{K}_i^{-1} \bar{\boldsymbol{u}}_i \qquad (4)$$

The objective of celestial triangulation is to use $n \geq 2$ LOS directions $\{\boldsymbol{\ell}_i\}_1^n$ to celestial bodies of known position (i.e., known $\{\boldsymbol{p}_i\}_1^n$) to infer the location of the observer. This describes the resection form of triangulation.[5] Moreover, since the attitude of the sensor is usually known (e.g., from stars in the same image(s) as the unresolved celestial bodies) the most common situation is an absolute triangulation problem.[5]

Optimal Triangulation. There are many popular methods of triangulation, but not all of them are statistically optimal. Some very common methods, such as the unweighted Direct Linear Transform (DLT)[7,8] or explicitly estimating range,[1,4] provide non-iterative solutions that can consider many measurements in the least-squares sense—however, the cost function used by the least-squares formulation does not minimize the covariance-weighted measurement residuals and so the result is not a maximum likelihood estimate (MLE). Depending on the geometry, this can result in localization errors an order of magnitude (or more) larger than using a statistically optimal triangulation algorithm.

Multiple methods for statistically optimal triangulation exist. When only two objects are observed, the classical result from Hartley and Sturm[9] offers an optimal triangulation as the solution to a polynomial of degree six. When both LOS measurements originate from a single

image, then the degree six polynomial can be simplified to a quadratic equation.[5,10,11] For more than two objects, the degree of the polynomial to solve quickly becomes intractable (e.g., polynomial of degree 47 for three objects[12]). Until recently, the main way to practically solve the optimal triangulation problem with more than two objects was with iterative optimization schemes.[7] In early 2022, however, Henry and Christian proposed a new non-iterative way to solve the statistically optimal problem called Linear Optimal Sine Triangulation (LOST).[5]

LOST Algorithm. Consider the perfect image plane coordinate $\bar{\boldsymbol{x}}_i$ (corresponding to the LOS direction $\boldsymbol{\ell}_i \propto \bar{\boldsymbol{x}}_i$) that points from the observer at $\boldsymbol{r}$ to an object at $\boldsymbol{p}_i$. Taking the cross product of Eq. (1) with this measurement (vector equivalent to law of sines), one obtains

$$[\bar{\boldsymbol{x}}_i \times]\, \boldsymbol{T}_{C_i}^I (\boldsymbol{r}_I - \boldsymbol{p}_{I_i}) = \boldsymbol{0}_{3 \times 1} \qquad (5)$$

where we have introduced specific frames and $\boldsymbol{T}_{C_i}^I$ is the transformation matrix from frame I (e.g., ICRF) to camera frame C_i frame. We index the camera frame by observation since we will have many LOS measurements and they may not all come from the same camera. Equation (5) also makes use of the 3×3 skew-symmetric matrix $[\cdot \times]$, which follows the convention $[\boldsymbol{a} \times]\boldsymbol{b} = \boldsymbol{a} \times \boldsymbol{b}$.

When the measurement is corrupted by additive noise $\boldsymbol{w}_i$ (the covariance for $\boldsymbol{w}_i$ is not full rank since $\bar{\boldsymbol{x}}_i$ is in homogeneous coordinates—see Ref. 5 for details),

$$\tilde{\bar{\boldsymbol{x}}}_i = \bar{\boldsymbol{x}}_i + \boldsymbol{w}_i \qquad (6)$$

we find that Eq. (5) no longer exactly equals zero

$$\begin{aligned} \boldsymbol{\epsilon}_i &= \left[\tilde{\bar{\boldsymbol{x}}}_i \times\right] \boldsymbol{T}_{C_i}^I (\boldsymbol{r}_I - \boldsymbol{p}_{I_i}) \\ &= \left[\boldsymbol{T}_{C_i}^I (\boldsymbol{p}_{I_i} - \boldsymbol{r}_I) \times\right] \tilde{\bar{\boldsymbol{x}}}_i \neq \boldsymbol{0}_{3 \times 1} \end{aligned} \qquad (7)$$

Assuming perfect knowledge of $\boldsymbol{p}_I$ (more on this later) and that $\boldsymbol{w}_i$ absorbs both image processing (centroiding)
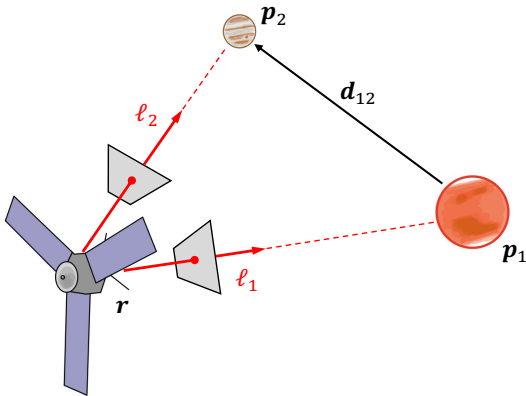

Figure 1. Absolute triangulation for spacecraft localization using the line-of-sight (LOS) to two celestial bodies.

and attitude error, the covariance of $\boldsymbol{\epsilon}_i$ is related to the measurement covariance $\boldsymbol{R}_{\bar{\boldsymbol{x}}_i} = E[\boldsymbol{w}_i \boldsymbol{w}_i^T]$ by

$$\boldsymbol{R}_{\boldsymbol{\epsilon}_i} = -\left[\boldsymbol{T}_{C_i}^I (\boldsymbol{p}_{I_i} - \boldsymbol{r}_I) \times\right] \boldsymbol{R}_{\bar{\boldsymbol{x}}_i} \left[\boldsymbol{T}_{C_i}^I (\boldsymbol{p}_{I_i} - \boldsymbol{r}_I) \times\right] \quad (8)$$

In order to obtain the maximum likelihood estimate, we seek to minimize the cost function

$$\min J(\boldsymbol{r}_I) = \sum_{i=1}^n \boldsymbol{\epsilon}_i^T \boldsymbol{R}_{\boldsymbol{\epsilon}_i}^{-1} \boldsymbol{\epsilon}_i \qquad (9)$$

The primary difficulty is computing $\boldsymbol{R}_{\boldsymbol{\epsilon}_i}$ when a good estimate of the position $\boldsymbol{r}_I$ is not known *a priori*. In Ref. 5, Henry and Christian show that an excellent approximation of $\boldsymbol{R}_{\boldsymbol{\epsilon}_i}$ may be computed as

$$\tilde{\boldsymbol{R}}_{\boldsymbol{\epsilon}_i} = -\gamma_i^2 \left[\tilde{\bar{\boldsymbol{x}}}_i \times\right] \boldsymbol{R}_{\bar{\boldsymbol{x}}_i} \left[\tilde{\bar{\boldsymbol{x}}}_i \times\right] \qquad (10)$$

where

$$\gamma_i = \frac{\tilde{\rho}_i}{\|\tilde{\bar{\boldsymbol{x}}}_i\|} = \frac{\|\boldsymbol{d}_{I_{ij}} \times \boldsymbol{T}_I^{C_j} \tilde{\bar{\boldsymbol{x}}}_j\|}{\|\boldsymbol{T}_I^{C_i} \tilde{\bar{\boldsymbol{x}}}_i \times \boldsymbol{T}_I^{C_j} \tilde{\bar{\boldsymbol{x}}}_j\|} \qquad (11)$$

where $\boldsymbol{d}_{I_{ij}} = \boldsymbol{p}_{I_j} - \boldsymbol{p}_{I_i}$. Since the positions of the planets are known from ephemeris files, it follows that $\boldsymbol{d}_{I_{ij}}$ is also a known vector.

The covariance expression in Eq. (10) is rank deficient (a 3×3 matrix of rank two). However, due to the structure of the problem (specifically, the null space direction of $[\tilde{\bar{\boldsymbol{x}}}_i \times]$) we may use the pseudoinverse to find the optimal solution in terms of the Normal equations[5]

$$\left(\sum_{i=1}^n \boldsymbol{T}_I^{C_i} \left[\tilde{\bar{\boldsymbol{x}}}_i \times\right] \tilde{\boldsymbol{R}}_{\boldsymbol{\epsilon}_i}^\dagger \left[\tilde{\bar{\boldsymbol{x}}}_i \times\right] \boldsymbol{T}_{C_i}^I\right) \hat{\boldsymbol{r}}_I = \\ \sum_{i=1}^n \boldsymbol{T}_I^{C_i} \left[\tilde{\bar{\boldsymbol{x}}}_i \times\right] \tilde{\boldsymbol{R}}_{\boldsymbol{\epsilon}_i}^\dagger \left[\tilde{\bar{\boldsymbol{x}}}_i \times\right] \boldsymbol{T}_{C_i}^I \boldsymbol{p}_{I_i} \qquad (12)$$

Considering isotropic centroiding error in an image, it is possible to define

$$q_i = \frac{1}{\sigma_{\boldsymbol{x}_i} \gamma_i} = \frac{\|\boldsymbol{T}_I^{C_i} \tilde{\bar{\boldsymbol{x}}}_i \times \boldsymbol{T}_I^{C_i} \tilde{\bar{\boldsymbol{x}}}_j\|}{\sigma_{\boldsymbol{x}_i} \|\boldsymbol{d}_{I_{ij}} \times \boldsymbol{T}_I^{C_j} \tilde{\bar{\boldsymbol{x}}}_j\|} \qquad (13)$$

and reformulate the problem into a nicely structured linear system that can be directly solved for $\boldsymbol{r}_I$

$$\begin{bmatrix} q_1 \boldsymbol{S} \left[\tilde{\bar{\boldsymbol{x}}}_1 \times\right] \boldsymbol{T}_{C_1}^I \\ q_2 \boldsymbol{S} \left[\tilde{\bar{\boldsymbol{x}}}_2 \times\right] \boldsymbol{T}_{C_2}^I \\ \vdots \\ q_n \boldsymbol{S} \left[\tilde{\bar{\boldsymbol{x}}}_n \times\right] \boldsymbol{T}_{C_n}^I \end{bmatrix} \boldsymbol{r}_I = \begin{bmatrix} q_1 \boldsymbol{S} \left[\tilde{\bar{\boldsymbol{x}}}_1 \times\right] \boldsymbol{T}_{C_1}^I \boldsymbol{p}_{I_1} \\ q_2 \boldsymbol{S} \left[\tilde{\bar{\boldsymbol{x}}}_2 \times\right] \boldsymbol{T}_{C_2}^I \boldsymbol{p}_{I_2} \\ \vdots \\ q_n \boldsymbol{S} \left[\tilde{\bar{\boldsymbol{x}}}_n \times\right] \boldsymbol{T}_{C_n}^I \boldsymbol{p}_{I_n} \end{bmatrix} \quad (14)$$

where $\boldsymbol{S} = [\boldsymbol{I}_{2\times2}, \boldsymbol{0}_{2\times1}]$. Finally, we remind the reader that $\tilde{\bar{\boldsymbol{x}}}_i = \boldsymbol{K}_i^{-1} \tilde{\boldsymbol{u}}_i$ and so $\tilde{\bar{\boldsymbol{x}}}_i$ can easily be constructed from the raw measurements $\tilde{\boldsymbol{u}}_i$ for a calibrated camera (i.e, when $\boldsymbol{K}_i$ is known). This section uses $\tilde{\bar{\boldsymbol{x}}}_i$ for compactness (whereas Ref. 5 uses $\boldsymbol{K}_i^{-1} \tilde{\boldsymbol{u}}_i$ to make the measurements appear more explicitly).

Planetary Ephemeris and Attitude Errors. Absolute triangulation algorithms (e.g., LOST) depend on the assumption that the attitude $\boldsymbol{T}_{C_i}^I$ and planet positions $\boldsymbol{p}_{I_i}$ are known. Thus, we find it helpful to study when it is important to consider how the uncertainty in these parameters affects the resulting triangulation solution.

The LOST method is fundamentally a maximum likelihood estimate that makes use of the pseudomeasurement $\boldsymbol{y}_i$ of the form

$$\boldsymbol{y}_i = [\bar{\boldsymbol{x}}_i\times]\,\boldsymbol{T}_{C_i}^I(\boldsymbol{r}_I - \boldsymbol{p}_{I_i}) = \boldsymbol{0}_{3\times1} \qquad (15)$$

with a noisy measurement given by

$$\tilde{\boldsymbol{y}}_i = \boldsymbol{y}_i + \boldsymbol{\epsilon}_i = \boldsymbol{\epsilon}_i \qquad (16)$$

If errors only exist in the image plane measurements $\bar{\boldsymbol{x}}_i$, then the covariance of $\boldsymbol{y}_i$ is the $\boldsymbol{R}_{\epsilon_i} = E[\boldsymbol{\epsilon}_i\boldsymbol{\epsilon}_i^T]$ used in the original LOST formulation that is given in Eq. (10).

Now, we briefly consider what happens when there are also errors in $\boldsymbol{T}_{C_i}^I$ and $\boldsymbol{p}_{I_i}$. To do this, take the partials

$$\boldsymbol{H}_{\bar{\boldsymbol{x}}_i} = \frac{\partial \boldsymbol{y}_i}{\partial \bar{\boldsymbol{x}}_i} = -\left[\boldsymbol{T}_{C_i}^I(\boldsymbol{r}_I - \boldsymbol{p}_{I_i})\times\right] = -\gamma_i\,[\bar{\boldsymbol{x}}_i\times] \quad (17)$$

$$\boldsymbol{H}_{\boldsymbol{\phi}_i} = \frac{\partial \boldsymbol{y}_i}{\partial \boldsymbol{\phi}_i} = [\bar{\boldsymbol{x}}_i\times]\left[\boldsymbol{T}_{C_i}^I(\boldsymbol{r}_I - \boldsymbol{p}_{I_i})\times\right] = \gamma_i\,[\bar{\boldsymbol{x}}_i\times]^2$$

$$\boldsymbol{H}_{\boldsymbol{p}_i} = \frac{\partial \boldsymbol{y}_i}{\partial \boldsymbol{p}_{I_i}} = -[\bar{\boldsymbol{x}}_i\times]\,\boldsymbol{T}_{C_i}^I$$

where $\boldsymbol{\phi}_i$ is the angle-vector description of an attitude perturbation in $\boldsymbol{T}_{C_i}^I$. This leads to the differential

$$\boldsymbol{\epsilon}_i = \boldsymbol{H}_{\bar{\boldsymbol{x}}_i}\boldsymbol{w}_i + \boldsymbol{H}_{\boldsymbol{\phi}_i}\delta\boldsymbol{\phi}_i + \boldsymbol{H}_{\boldsymbol{p}_{I_i}}\delta\boldsymbol{p}_{I_i} \qquad (18)$$

Assuming the various errors are uncorrelated, we may compute the complete covariance $\boldsymbol{R}_{\epsilon_i} = [\boldsymbol{\epsilon}_i\boldsymbol{\epsilon}_i^T]$ as

$$\boldsymbol{R}_{\epsilon_i} = \boldsymbol{H}_{\bar{\boldsymbol{x}}_i}\boldsymbol{R}_{\bar{\boldsymbol{x}}_i}\boldsymbol{H}_{\bar{\boldsymbol{x}}_i}^T + \boldsymbol{H}_{\boldsymbol{\phi}_i}\boldsymbol{R}_{\boldsymbol{\phi}_i}\boldsymbol{H}_{\boldsymbol{\phi}_i}^T + \boldsymbol{H}_{\boldsymbol{p}_{I_i}}\boldsymbol{R}_{\boldsymbol{p}_{I_i}}\boldsymbol{H}_{\boldsymbol{p}_{I_i}}^T \qquad (19)$$

which is

$$\boldsymbol{R}_{\epsilon_i} = -\gamma_i^2\,[\bar{\boldsymbol{x}}_i\times]\left(\boldsymbol{R}_{\bar{\boldsymbol{x}}_i} - [\bar{\boldsymbol{x}}_i\times]\,\boldsymbol{R}_{\boldsymbol{\phi}_i}\,[\bar{\boldsymbol{x}}_i\times]\right)[\bar{\boldsymbol{x}}_i\times] \quad (20)$$
$$- [\bar{\boldsymbol{x}}_i\times]\,\boldsymbol{T}_{C_i}^I\boldsymbol{R}_{\boldsymbol{p}_{I_i}}\boldsymbol{T}_I^{C_i}\,[\bar{\boldsymbol{x}}_i\times]$$

where we note the leading negative sign comes from the identity $[\bar{\boldsymbol{x}}_i\times]^T = -[\bar{\boldsymbol{x}}_i\times]$. Additionally, that errors from $\bar{\boldsymbol{x}}_i$ and $\boldsymbol{\phi}_i$ can be grouped together as shown here is why it was stated earlier that errors from centroiding and attitude can be combined within the original LOST cost function. Thus, letting $\boldsymbol{R}'_{\bar{\boldsymbol{x}}_i} = \boldsymbol{R}_{\bar{\boldsymbol{x}}_i} - [\bar{\boldsymbol{x}}_i\times]\,\boldsymbol{R}_{\boldsymbol{\phi}_i}\,[\bar{\boldsymbol{x}}_i\times]$ be the combined centroiding and attitude error covariance, we have

$$\boldsymbol{R}_{\epsilon_i} = -[\bar{\boldsymbol{x}}_i\times]\left(\gamma_i^2\boldsymbol{R}'_{\bar{\boldsymbol{x}}_i} + \boldsymbol{T}_{C_i}^I\boldsymbol{R}_{\boldsymbol{p}_{I_i}}\boldsymbol{T}_I^{C_i}\right)[\bar{\boldsymbol{x}}_i\times] \quad (21)$$

To determine if (when?) the error in $\boldsymbol{p}_{I_i}$ is important, we consider the relative size of the terms within the parentheses in Eq. (21). Consider first the covariance

matrix $\boldsymbol{R}'_{\bar{\boldsymbol{x}}_i}$. Since $\bar{\boldsymbol{x}}_i^T = [x_i, y_i, 1]$, the covariance is rank deficient (the third element is exactly one and has no uncertainty), and so for isotropic image noise $\sigma_{\bar{\boldsymbol{x}}_i}$ we find

$$\boldsymbol{R}_{\bar{\boldsymbol{x}}_i} \approx \sigma_{\bar{\boldsymbol{x}}_i}^2 \begin{bmatrix} 1 & 0 & 0 \\ 0 & 1 & 0 \\ 0 & 0 & 0 \end{bmatrix} \qquad (22)$$

Moreover, for a modest field-of-view (FOV) camera we find $\|\bar{\boldsymbol{x}}_i\| \approx 1$ such that Eq. (11) leads to $\gamma_i \approx \rho_i$. Considering attitude error with covariance $\boldsymbol{R}_{\boldsymbol{\phi}_i} = \sigma_{\boldsymbol{\phi}_i}^2\boldsymbol{I}_{3\times3}$ the narrow FOV assumption also leads to

$$[\bar{\boldsymbol{x}}_i\times]\,\boldsymbol{R}_{\boldsymbol{\phi}_i}\,[\bar{\boldsymbol{x}}_i\times] \approx -\sigma_{\boldsymbol{\phi}_i}^2 \begin{bmatrix} 1 & 0 & 0 \\ 0 & 1 & 0 \\ 0 & 0 & 0 \end{bmatrix} \qquad (23)$$

If stars in the same image were used to compute attitude then a conservative approximation is $\sigma_{\bar{\boldsymbol{x}}_i} \approx \sigma_{\boldsymbol{\phi}_i}$, and we arrive at a simple approximation for $\boldsymbol{R}'_{\bar{\boldsymbol{x}}_i}$

$$\boldsymbol{R}'_{\bar{\boldsymbol{x}}_i} = \boldsymbol{R}_{\bar{\boldsymbol{x}}_i} - [\bar{\boldsymbol{x}}_i\times]\,\boldsymbol{R}_{\boldsymbol{\phi}_i}\,[\bar{\boldsymbol{x}}_i\times] \approx 2\sigma_{\bar{\boldsymbol{x}}_i}^2 \begin{bmatrix} 1 & 0 & 0 \\ 0 & 1 & 0 \\ 0 & 0 & 0 \end{bmatrix} \quad (24)$$

Thus, we can approximate the size of the first term within the parentheses of Eq. (21) as

$$\text{Tr}[\gamma_i^2\boldsymbol{R}'_{\bar{\boldsymbol{x}}_i}] \approx 4\sigma_{\bar{\boldsymbol{x}}_i}^2\rho_i^2 \qquad (25)$$

where $\text{Tr}[\cdot]$ is the trace operator. Likewise, assuming an isotropic position uncertainty in a planet's location $\boldsymbol{R}_{\boldsymbol{p}_{I_i}} = \sigma_{\boldsymbol{p}_i}^2\boldsymbol{I}_{3\times3}$, we see that the covariance has a size

$$\text{Tr}[\boldsymbol{T}_{C_i}^I\boldsymbol{R}_{\boldsymbol{p}_{I_i}}\boldsymbol{T}_I^{C_i}] \approx 3\sigma_{\boldsymbol{p}_i}^2 \qquad (26)$$

We argue here that it is possible to neglect the position uncertainty of the planet whenever it is comparatively small. This leads to the condition

$$\text{Tr}[\gamma_i^2\boldsymbol{R}'_{\bar{\boldsymbol{x}}_i}] \gg \text{Tr}[\boldsymbol{T}_{C_i}^I\boldsymbol{R}_{\boldsymbol{p}_{I_i}}\boldsymbol{T}_I^{C_i}] \qquad (27)$$

Or, equivalently,

$$4\sigma_{\bar{\boldsymbol{x}}_i}^2\rho_i^2 \gg 3\sigma_{\boldsymbol{p}_i}^2 \quad \rightarrow \quad \sigma_{\bar{\boldsymbol{x}}_i}^2\rho_i^2 \gg \sigma_{\boldsymbol{p}_i}^2 \qquad (28)$$

Thus, we do *not* have to consider planetary ephemeris error at "large" ranges ρ_i, where large is defined as

$$\rho_i \gg \sigma_{\boldsymbol{p}_i}/\sigma_{\bar{\boldsymbol{x}}_i} \qquad (29)$$

This result agrees with geometric intuition, as illustrated in Fig. 2.

Typical numerical values can be attributed to the parameters to study the practical implications for celestial navigation. Consider the medium-resolution camera from Ref. 13 with an IFOV of $60\mu\text{rad}$ (≈ 12 arcsec) and a pixel standard deviation 0.1 pixel, leading to a focal plane error of $\sigma_{\boldsymbol{x}_i} = 6 \times 10^{-6}$ (≈ 1.2 arcsec). The planet uncertainties are coarsely approximated at year 2030 from the data in Ref. 14 and are tabulated in Table 1. Also shown

in this table are the ranges beyond which these planetary ephemeris uncertainties cease to matter as compared to centroiding errors of $\sigma_{\boldsymbol{x}_i}$. The "much greater than" threshold is taken to be an order of magnitude, so we compute this critical range as $\rho_i \approx 10\sigma_{\boldsymbol{p}_i}/\sigma_{\boldsymbol{x}_i} \approx 1.7\times 10^6 \sigma_{\boldsymbol{p}_{I_i}}$. From Table 1 we see that planetary ephemeris error is only important when navigating in close proximity to the planets. We also observe that the ranges for planet-based celestial navigation within the Solar System are typically on the order of 1 astronomical unit (AU) or more, and so planetary ephemeris error is usually not a major contributor to triangulation error.

In the unusual event that planetary ephemeris error must be considered, one may simply use Eq. (20) for $\boldsymbol{R}_{\boldsymbol{\epsilon}_i}$ within the Normal equations version of the LOST algorithm given in Eq. (12). This will automatically perform non-iterative triangulation with the statistically optimal consideration of LOS direction errors ($\sigma_{\bar{\boldsymbol{x}}_i}$), range to the observed bodies (ρ_i), attitude errors ($\sigma_{\boldsymbol{\phi}_i}$), and planetary ephemeris errors ($\sigma_{\boldsymbol{p}_{I_i}}$). No further modifications are necessary.

Aberration of Light. The apparent direction of an incoming ray of light depends on the velocity of the observer. This effect has been known since at least the 1700s (famously by Bradley[15]) and was a major motivation for Einstein's original study of relativity. The modern explanation is due to Einstein's Special Theory of Relativity, with the key (scalar) equation appearing on pg. 912 of his seminal 1905 paper,[16]

$$\cos\phi' = \frac{\cos\phi - (v/c)}{1 - (v/c)\cos\phi} \qquad (30)$$

where $v = \|\boldsymbol{v}\|$ is the observer's speed and c is the speed of light. Additionally, we define ϕ as the angle between
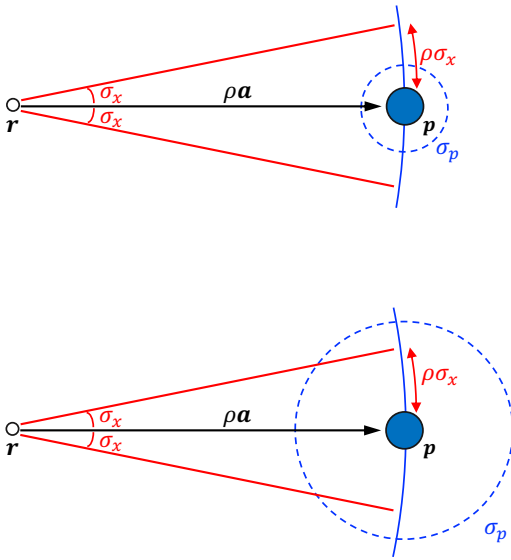

Figure 2. The position uncertainty of the celestial body can only be ignored when $\rho\sigma_{\mathbf{x}} \gg \sigma_{\mathbf{p}}$.

Planet	$\sigma_{\mathbf{p}_{I_i}}$ (km)	critical range, ρ_i (km)	(AU)
Mercury	1.4	2.267×10^6	0.015
Venus	0.5	9.014×10^5	0.006
Mars	8.6	1.436×10^7	0.096
Jupiter	28.4	4.741×10^7	0.317
Saturn	7.3	1.214×10^7	0.081
Uranus	531.5	8.859×10^8	5.922
Neptune	1500.0	2.500×10^9	16.71

incoming ray of light (opposite direction as the LOS vector) and the velocity vector in the rest frame. The angle ϕ' is the same thing as it appears to someone in the frame of the moving observer. Einstein's original equation has everything we need, though it is often convenient for spacecraft navigators to express this in vector form.[17]

Despite Einstein's lucid description of this phenomenon and over 100 years of precedence, there remains great confusion over the application of this concept. Indeed, many contemporary authors of celestial triangulation continue to pass along incorrect models for this effect—potentially with disastrous results if these algorithms were ever to be implemented outside of academic papers.

The most pervasive misconception is that light aberration depends on the relative velocity between the source (e.g., planet) and the observer (e.g., camera on a spacecraft). This is not true. Alterations in the apparent direction only depend on the velocity of the observer. This mistake is nicely explained in a "question-and-answer" exchange in *Nature* from 1949 (question by C.O. Hines and answer by R. d'E. Atkinson).[18]

The second (and less serious) mistake is the fixation on high(er) precision in the correction for aberration due to the velocity of the observer, without regard for gravitational deflection of light of similar magnitude due to the General Theory of Relativity (also thanks to Einstein). A nice overview of the entire procedure for correcting optical planetary observations is given by Kaplan in Ref. 19. A discussion of these same ideas with a notation friendly for spacecraft navigators may be found in Ref. 17

The third mistake is correcting for aberration when no correction is necessary. For most astronomical cameras and star trackers, the sensor field-of-view (FOV) is relatively small. If a planet LOS is constructed from such an image and stars in this same image are used to compute the ICRF-to-camera attitude (as is often the case), then it is often the case that no correction for aberration is necessary since similar aberrations are experienced by every source (planets and stars) within the image. Consequently, the effect of aberration on the star observations cancels the effect of aberration on the planet observation when constructing an ICRF LOS direction.

We now briefly develop the correct models for aberration and show how intelligent system design may be used to remove this effect from the problem entirely. Suppose we have a unit vector $\boldsymbol{a}_i$ in the direction $\boldsymbol{\ell}_i$, such that

$$\boldsymbol{a}_i \propto \boldsymbol{\ell}_i \propto \boldsymbol{p}_i - \boldsymbol{r} = \rho_i \boldsymbol{a}_i \qquad (31)$$

where ρ_i is the distance between the observer at $\boldsymbol{r}$ and the observed object at $\boldsymbol{p}_i$. Recall from before that $\boldsymbol{p}_i$ is the location of the planet when the light left it, which is different from the planet's location at the time of observation (light time-of-flight effects are discussed in a different section of this paper). All of the quantities in Eq. (31) are expressed in the rest frame (e.g., ICRF). Now, proceed by rewriting Einstein's result from Eq. (30) in vector form[17, 20]

$$\boldsymbol{a}_i' = \boldsymbol{a}_i + [\boldsymbol{a}_i \times (\boldsymbol{\beta} \times \boldsymbol{a}_i)] + \mathcal{O}(\|\boldsymbol{\beta}\|^2) \qquad (32)$$

where $\boldsymbol{a}_i'$ is the LOS unit vector as seen by an observer moving with velocity $\boldsymbol{v}$ relative to the rest frame. Following the usual conventions, we denote velocity as a fraction of the speed of light as $\boldsymbol{\beta} = \boldsymbol{v}/c$ for notational compactness.

Because spacecraft travel at speeds that are small compared to the speed of light, the first order term in $\boldsymbol{\beta}$ of Eq. (32) will always dominate the higher order terms. The second order term can still lead to changes in the mas range,[17] but that is neglected here since most OP-NAV instruments achieve only arcsecond-level LOS errors (at best). Thus, retaining only first-order terms from Eq. (32),

$$\boldsymbol{a}_i' \approx (\boldsymbol{I}_{3\times 3} - [(\boldsymbol{\beta} \times \boldsymbol{a}_i)\times]) \, \boldsymbol{a}_i \qquad (33)$$

Now, recall the small angle approximation (to first order) for an attitude transformation

$$\Delta \boldsymbol{T}_i \approx \boldsymbol{I}_{3\times 3} - [\Delta\boldsymbol{\theta}_i\times] \qquad (34)$$

where $\Delta\boldsymbol{\theta}$ is an angle vector.[21] Thus, the aberration effect in Eq. (33) acts as a rotation on the unit vector $\boldsymbol{a}_i$ by the angle vector $\Delta\boldsymbol{\theta}_i$

$$\Delta\boldsymbol{\theta}_i = \boldsymbol{\beta} \times \boldsymbol{a}_i \qquad (35)$$

This rotation preserves the unit vector length to first order. We may therefore relate the inertial unit vector $\boldsymbol{a}_{I_i}$ to the apparent direction (after aberration) in the camera frame by

$$\boldsymbol{a}_i' \approx \boldsymbol{T}_C^I \boldsymbol{a}_{I_i}' = \boldsymbol{T}_C^I \, \Delta\boldsymbol{T} \, \boldsymbol{a}_{I_i} \qquad (36)$$

where we once again use no subscripts to indicate the camera frame. Observe that the change in LOS direction given by $\Delta\boldsymbol{\theta}_i$ depends only on the observer's velocity (and *not* on the observed planet's velocity) and is entierely unaffected by the range ρ_i.

Consequently the change in bearing direction is limited by

$$\Delta\theta_i \approx \|\boldsymbol{\beta} \times \boldsymbol{a}_i\| \leq \|\boldsymbol{\beta}\| \qquad (37)$$

with the maximum perturbation occurring when the LOS direction is perpendicular to the observer velocity. Some example light aberration maximums (to first order) at typical spacecraft speeds within the Solar System are provided in Table 2.

The aberration angles in Table 2 are all large enough to matter for spacecraft celestial triangulation—and so it might seem reasonable to correct for this effect. The important thing to remember, however, is that these angles are perturbations relative to the rest frame (ICRF) and only matter if you independently know the sensor attitude relative to ICRF *without aberration*.

Suppose that we have a camera with a modest FOV. Consider the case where the image contains a planet and stars, with the planet LOS being used for triangulation and the stars used to determine the image attitude. If the stars have inertial direction $\boldsymbol{e}_{I_i}$, they may be transformed (for a stationary observer) into the camera frame according to

$$\boldsymbol{e}_j = \boldsymbol{T}_C^I \boldsymbol{e}_{I_j} \qquad (38)$$

where we once again use no subscripts to indicate the camera frame. Accounting for light aberration due to the observer's motion, the transformation becomes

$$\boldsymbol{e}_j' = \boldsymbol{T}_C^I \, \Delta\boldsymbol{T}_j \, \boldsymbol{e}_{I_j} = \boldsymbol{T}_C^I \boldsymbol{e}_{I_j}' \qquad (39)$$

If a set of unit vector pairs $\{\boldsymbol{e}_j', \boldsymbol{e}_{I_j}\}_1^n$ are used to solve Whaba's problem,[21, 22] the result is an attitude estimate $\tilde{\boldsymbol{T}}_C^I \approx \boldsymbol{T}_C^I\Delta\boldsymbol{T}$, where $\Delta\boldsymbol{T}$ is some average of the various contributing $\Delta\boldsymbol{T}_j$ (the specific equation may be written, but isn't important here). If we observe a planet direction $\boldsymbol{a}_i'$, we would want to use the attitude from the stars in the same image to get the LOS in the inertial frame: $\tilde{\boldsymbol{T}}_I^C \boldsymbol{a}_i'$. Therefore, substituting for $\boldsymbol{a}_i'$ from Eq. (36) and also $\tilde{\boldsymbol{T}}_C^I \approx \boldsymbol{T}_C^I\Delta\boldsymbol{T}$,

$$\begin{aligned}
\tilde{\boldsymbol{T}}_I^C \boldsymbol{a}_i' &= \left(\tilde{\boldsymbol{T}}_C^I\right)^T \boldsymbol{a}_i' \\
&\approx \left(\boldsymbol{T}_C^I\Delta\boldsymbol{T}\right)^T \boldsymbol{T}_C^I\Delta\boldsymbol{T}_i \boldsymbol{a}_{I_i} \\
&= (\Delta\boldsymbol{T})^T \left(\boldsymbol{T}_C^I\right)^T \boldsymbol{T}_C^I\Delta\boldsymbol{T}_i \boldsymbol{a}_{I_i} \\
&= \Delta\boldsymbol{T}^T \Delta\boldsymbol{T}_i \boldsymbol{a}_{I_i}
\end{aligned}$$

Consider the term $\Delta\boldsymbol{T}^T \Delta\boldsymbol{T}_i$ more carefully,

$$\begin{aligned}
\Delta\boldsymbol{T}^T \Delta\boldsymbol{T}_i &= (\boldsymbol{I}_{3\times 3} - [\Delta\boldsymbol{\theta}\times])^T (\boldsymbol{I}_{3\times 3} - [\Delta\boldsymbol{\theta}_i\times]) \\
&= \boldsymbol{I}_{3\times 3} + [\Delta\boldsymbol{\theta}\times] - [\Delta\boldsymbol{\theta}_i\times] - [\Delta\boldsymbol{\theta}\times][\Delta\boldsymbol{\theta}_i\times] \\
&\approx \boldsymbol{I}_{3\times 3} + [\Delta\boldsymbol{\theta}\times] - [\Delta\boldsymbol{\theta}_i\times] \\
&= \boldsymbol{I}_{3\times 3} - [(\Delta\boldsymbol{\theta}_i - \Delta\boldsymbol{\theta})\times]
\end{aligned}$$

where he have kept only first order terms in $\Delta\theta$ (which is equivalent to keeping only first order in $\boldsymbol{\beta} = \boldsymbol{v}/c$). This means the apparent rotation caused by $\Delta\boldsymbol{T}^T \Delta\boldsymbol{T}_i$ corresponds to the angle $\Delta\boldsymbol{\theta}_i - \Delta\boldsymbol{\theta}$. Now, consider this angle

Table 2. *Maximum light aberration with ($\Delta\theta$) and without ($\Delta\psi$) externally determined attitude at velocities of some space missions. Actual aberrations are often much smaller.*

| | | | $\Delta\psi$ (arcsec) | |
| | | | mid-resolution | high-resolution |
Example Orbit	$\|\boldsymbol{v}\|$ (km/s)	$\Delta\theta$ (arcsec)	FOV = 7 deg	FOV = 0.6 deg
Earth LEO	37.7	25.92	1.58	0.136
Earth GEO	32.9	22.62	1.28	0.118
Cassini (max)	44.0	30.27	1.85	0.159
Parker Solar Probe (max yet)	163.0	112.15	6.85	0.587

further. Substitute from Eq. (35) to find

$$\Delta\boldsymbol{\psi}_i = \Delta\boldsymbol{\theta}_i - \Delta\boldsymbol{\theta} = (\boldsymbol{\beta} \times \boldsymbol{a}_i) - (\boldsymbol{\beta} \times \boldsymbol{e}) \tag{40}$$
$$= \boldsymbol{\beta} \times (\boldsymbol{a}_i - \boldsymbol{e}) \tag{41}$$

where $\boldsymbol{e}$ roughly corresponds to the "average" direction of the stars used to compute $\tilde{\boldsymbol{T}}_C^I$. We can compute the magnitude of this change as

$$\|\Delta\boldsymbol{\psi}_i\| = \|\boldsymbol{\beta} \times (\boldsymbol{a}_i - \boldsymbol{e})\| \leq \|\boldsymbol{\beta}\| \, \|\boldsymbol{a}_i - \boldsymbol{e}\| \tag{42}$$

Substituting this into the above, we find that this angle describes the error in our estimated inertial LOS direction

$$\tilde{\boldsymbol{a}}_{I_i} = (\boldsymbol{I}_{3\times3} - [\Delta\boldsymbol{\psi}_i]) \, \boldsymbol{a}'_{I_i} = \tilde{\boldsymbol{T}}_I^C \boldsymbol{a}'_i \tag{43}$$

If we assume $\boldsymbol{e}$ is somewhere around the center of the image, then the maximum angle $\Delta\phi_i$ occurs when $\boldsymbol{a}_{I_i}$ is near the edge of the image. Most OPNAV cameras have a small FOV. For example, consider the OPNAV cameras capable of providing arcsecond-level (or better) bearings from Ref. 2. For the medium-resolution camera with a (circular) FOV of 7 deg FOV, the angle between $\boldsymbol{e}$ and $\boldsymbol{a}_i$ can be no more than about 3.5 deg which corresponds to $\|\boldsymbol{e} - \boldsymbol{a}_i\| \approx 0.061$. The high-resolution camera has an even narrow FOV of 0.6 deg, leading to a maximum $\|\boldsymbol{e} - \boldsymbol{a}_i\| \approx 0.0052$. The resulting bearing errors $\Delta\psi$ values for some example orbits are summarized in Table 2. The primary result is that the effect of (special) relativistic light aberration on the ICRF planet LOS direction is usually not important with conventional navigation cameras when the image attitude is computed with stars from the same image. Future sensors that are more capable than what we fly today or ultra-high precision applications may require this effect to be explicitly modeled, which can be done by analytically correcting (to first order in $\boldsymbol{\beta} = \boldsymbol{v}/c$) the star and/or planet LOS directions by manipulation of Eq. (33),

$$\boldsymbol{a}_i \approx \left(\boldsymbol{I}_{3\times3} + \left[(\boldsymbol{\beta} \times \boldsymbol{a}'_i)\times\right]\right) \boldsymbol{a}'_i \tag{44}$$
$$\boldsymbol{e}_j \approx \left(\boldsymbol{I}_{3\times3} + \left[(\boldsymbol{\beta} \times \boldsymbol{e}'_j)\times\right]\right) \boldsymbol{e}'_j \tag{45}$$

These corrections are easy to apply, though they are not necessary with most of today's OPNAV sensors for the reasons discussed above.

Light Time-of-Flight. Light time-of-flight is important for celestial triangulation due to the very large distances involved. Since the planets are not stationary, the planet's location when the measurement is collected by the spacecraft is different from where it was when the observed photons left the body.

As before, denote the location of the observed planet when it reflects the observed photons as $\boldsymbol{p}_i$. After a time Δt_i these photons arrive at the spacecraft at location $\boldsymbol{r}$. It follows, therefore, that the distance traveled by the light is

$$\rho_i = \|\boldsymbol{p}_i - \boldsymbol{r}\| \tag{46}$$

and that the time Δt required to traverse this distance is given by

$$\Delta t_i = \rho_i/c \tag{47}$$

The principal difficulty here is that Δt is not known *a priori*. This creates a problem since we cannot directly recover $\boldsymbol{p}_i$ from our planetary ephemeris files since we do not (yet) know the correct time to query. Instead, we only know the time of the observation. Denote $\boldsymbol{p}_i^+$ as the location of the planet at the observation time.

Suppose that the velocity of the ith planet is given by $\boldsymbol{v}_i$ and is approximately constant over the time interval Δt_i. In this case, we see that

$$\boldsymbol{p}_i^+ \approx \boldsymbol{p}_i + \Delta t_i \, \boldsymbol{v}_i \tag{48}$$

Under these simplified dynamics we can develop a few useful analytical results. First, we can bound the change-in-range that light time-of-flight can cause for any particular planet. Second, we can quantify the change in LOS direction and then find a way to analytically compensate for this in closed-form within the optimal LOST framework.

Range effects. Begin by considering the effect of light time-of-flight on range. If the range were to be computed at the measurement time, one would find

$$\begin{aligned}
\rho_i'^2 &= \|\boldsymbol{p}_i^+ - \boldsymbol{r}\|^2 \\
&= (\boldsymbol{p}_i + \Delta t \boldsymbol{v}_i - \boldsymbol{r})^T (\boldsymbol{p}_i + \Delta t \boldsymbol{v}_i - \boldsymbol{r}) \\
&= \|\boldsymbol{p}_i - \boldsymbol{r}\|^2 + 2\Delta t \boldsymbol{v}_i^T (\boldsymbol{p}_i - \boldsymbol{r}) + \Delta t^2 \|\boldsymbol{v}_i\|^2 \\
&= \rho_i^2 + 2\Delta t \boldsymbol{v}_i^T (\boldsymbol{p}_i - \boldsymbol{r}) + \Delta t^2 \|\boldsymbol{v}_i\|^2
\end{aligned} \tag{49}$$

Substitution $\Delta t = \rho_i/c$ from Eq. (47) and $\boldsymbol{\beta}_i = \boldsymbol{v}_i/c$,

$$\begin{aligned}
\rho_i'^2 &= \rho_i^2 + 2\rho_i \boldsymbol{\beta}_i^T (\boldsymbol{p}_i - \boldsymbol{r}) + \rho_i^2 \|\boldsymbol{\beta}^2\|^2 \\
&= \rho_i^2 (1 + 2\boldsymbol{\beta}_i^T \boldsymbol{a}_i + \|\boldsymbol{\beta}_i\|^2)
\end{aligned} \tag{50}$$

where we once again use the notation $\boldsymbol{a}_i = \boldsymbol{\ell}_i/\|\boldsymbol{\ell}_i\|$ as the unit vector LOS. Denote the scale factor α as

$$\alpha_i = \sqrt{1 + 2\boldsymbol{\beta}_i^T \boldsymbol{a}_i + \|\boldsymbol{\beta}_i\|^2} \qquad (51)$$

such that

$$\rho_i' = \alpha_i \rho_i \qquad (52)$$

Given that the planet speeds are relatively low compared to the speed of light, we find that $\|\boldsymbol{\beta}\|^2 \ll \|\boldsymbol{\beta}\| \ll 1$. Observe now that the term $2\boldsymbol{\beta}_i^T \boldsymbol{a}_i$ has a magnitude of zero if the velocity is perpendicular to the LOS; and it reaches a maximum magnitude of $2\|\boldsymbol{\beta}_i\|$ when the velocity is *parallel* to the LOS. Thus, the scale factor α_i is bounded by

$$\alpha_i \le \alpha_{i,max} = \sqrt{1 + 2\|\boldsymbol{\beta}_i\| + \|\boldsymbol{\beta}_i\|^2} = 1 + \|\boldsymbol{\beta}\| \quad (53)$$

Thus the differences between the maximum scale factor and unity for the planets of the solar system are presented in Table 3 in the column $\|\boldsymbol{\beta}\|$. At those speeds, it is observed that $\alpha_{max} \approx 1$, indicating that $\rho_i' \approx \rho_i$. This states that the change in range is very small as compared to the overall range—a fact that is very important in analytical analysis.

Directional effects. The light time-of-flight is a measurable and important effect for most planets in our Solar System (especially the fast-moving inner planets). This will now be quantified and an analytic compensation will be derived.

Suppose we were to ignore light time-of-flight and compute the LOS direction from the spacecraft to the planet at the time of observation. Denote the resulting LOS direction as $\boldsymbol{\ell}_i'$ that is given by

$$\boldsymbol{\ell}_i' \propto \boldsymbol{p}_i^+ - \boldsymbol{r} \qquad (54)$$

The actual LOS direction is given by $\boldsymbol{\ell}_i$ from Eq. (1) and points towards where the planet was at a time Δt_i before the camera image was taken. The angular difference between $\boldsymbol{\ell}_i$ and $\boldsymbol{\ell}_i'$ is small, and so

$$\begin{aligned} \Delta\theta_i \approx \sin\Delta\theta_i &= \frac{\|\boldsymbol{\ell}_i' \times \boldsymbol{\ell}_i\|}{\|\boldsymbol{\ell}_i'\|\|\boldsymbol{\ell}_i\|} \\ &= \frac{\|(\boldsymbol{p}_i + \Delta t_i \boldsymbol{v}_i - \boldsymbol{r}) \times (\boldsymbol{p}_i - \boldsymbol{r})\|}{\|\rho_i'\|\|\rho_i\|} \\ &= \frac{\|(\Delta t_i \boldsymbol{v}_i) \times (\boldsymbol{p}_i - \boldsymbol{r})\|}{\rho_i' \rho_i} \\ &= (\Delta t_i/\rho_i')\|\boldsymbol{v}_i \times \boldsymbol{a}_i\| \end{aligned} \qquad (55)$$

Due to the cross product, the numerator of this expression is only influenced by the velocity perpendicular to the LOS. Additionally, we saw in the previous subsection that $\rho_i' \approx \rho_i$ at the velocities of interest. Therefore

$$\Delta\theta_i \approx (\Delta t_i/\rho_i)\|\boldsymbol{v}_{i,\perp}\| \qquad (56)$$

where $\boldsymbol{v}_\perp$ is the velocity perpendicular to the LOS direction: $\boldsymbol{v}_\perp = (\boldsymbol{I}_3 - \boldsymbol{a}\boldsymbol{a}^T)\boldsymbol{v}$. Substitution for Δt_i from Eq. (47) gives

$$\Delta\theta_i \approx \frac{\rho_i/c}{\rho_i}\|\boldsymbol{v}_{i,\perp}\| = \frac{\|\boldsymbol{v}_{i,\perp}\|}{c} = \|\boldsymbol{\beta}_{i,\perp}\| \le \|\boldsymbol{\beta}_i\| \quad (57)$$

The largest perturbation occurs when the planet is moving perpendicular to the LOS and $\boldsymbol{v} = \boldsymbol{v}_\perp$. In that case, we have $\Delta\theta \approx \|\boldsymbol{v}/c\| = \|\boldsymbol{\beta}\|$ and so the worst case perturbation in apparent direction due to time of light travel is given in Table 3. The perturbation will almost always be less, sometime substantially so.

The problem of light time-of-flight is then that the measured LOS is $\boldsymbol{\ell}_i$, but we have not yet found the position of the object at the time it emitted the photon, $\boldsymbol{p}_i$. We find that an excellent approximation of the time Δt_i may be found using the LOST range equation (obtained by manipulation of Eq. (11)). This will now be explored and the algorithmic benefits discussed.

To begin, consider perfect range estimation with the LOST range equation. To do this, use the LOS direction $\boldsymbol{\ell}_i$ and the position of the planets where they were when the light left

$$\rho_i = \frac{\|\boldsymbol{\ell}_i\| \|\boldsymbol{d}_{ij} \times \boldsymbol{\ell}_j\|}{\|\boldsymbol{\ell}_i \times \boldsymbol{\ell}_j\|} \qquad (58)$$

$$= \frac{\|\boldsymbol{\ell}_i\| \|(\boldsymbol{p}_j - \boldsymbol{p}_i) \times \boldsymbol{\ell}_j\|}{\|\boldsymbol{\ell}_i \times \boldsymbol{\ell}_j\|} \qquad (59)$$

where $\boldsymbol{d}_{ij} = \boldsymbol{p}_j - \boldsymbol{p}_i$. Now, we can instead use the current positions $\boldsymbol{p}_i' = \boldsymbol{p}_i + \Delta t_i \boldsymbol{v}_i$ of the planets to get an estimate of the light time-of-flight and range

$$c\Delta\hat{t}_i \approx \hat{\rho}_i \qquad (60)$$

$$= \frac{\|\boldsymbol{\ell}_i\| \|\boldsymbol{d}_{ij}' \times \boldsymbol{\ell}_j\|}{\|\boldsymbol{\ell}_i \times \boldsymbol{\ell}_j\|} \qquad (61)$$

$$= \frac{\|\boldsymbol{\ell}_i\| \|(\boldsymbol{p}_j' - \boldsymbol{p}_i') \times \boldsymbol{\ell}_j\|}{\|\boldsymbol{\ell}_i \times \boldsymbol{\ell}_j\|} \qquad (62)$$

$$= \frac{\|\boldsymbol{\ell}_i\| \|(\boldsymbol{p}_j - \boldsymbol{p}_i) \times \boldsymbol{\ell}_j + (\Delta t_j \boldsymbol{v}_j - \Delta t_i \boldsymbol{v}_i) \times \boldsymbol{\ell}_j\|}{\|\boldsymbol{\ell}_i \times \boldsymbol{\ell}_j\|} \qquad (63)$$

Suppose now that we have comparable light time-of-flights Δt_i and Δt_j. From the triangle inequality, we know that

$$\rho_i - \phi \le c\Delta\hat{t}_i \le \rho_i + \phi \qquad (64)$$

where

$$\phi = \frac{\|\boldsymbol{\ell}_i\|\|\Delta t_i(\boldsymbol{v}_j - \boldsymbol{v}_i) \times \boldsymbol{\ell}_j\|}{\|\boldsymbol{\ell}_i \times \boldsymbol{\ell}_j\|} \le \Delta t\|\boldsymbol{v}_j - \boldsymbol{v}_i\| \qquad (65)$$

And so

$$\|\Delta\hat{t} - \Delta t\| \le \Delta t\|\boldsymbol{\beta}_j - \boldsymbol{\beta}_i\| \qquad (66)$$

Following a similar procedure as before, the angular error of the corrected LOS is bounded by

$$\Delta\theta_i^{LOST} \approx \frac{\|\boldsymbol{v}_{i,\perp}(\Delta\hat{t} - \Delta t)\|}{\rho_i} \qquad (67)$$

$$\le \frac{\|\boldsymbol{v}_{i,\perp}\Delta t\|\boldsymbol{\beta}_j - \boldsymbol{\beta}_i\|\|}{\rho_i} \qquad (68)$$

$$= \|\boldsymbol{\beta}_{i,\perp}\|\|\boldsymbol{\beta}_j - \boldsymbol{\beta}_i\| \qquad (69)$$

Table 3. Summary of light time-of-flight effects on range and LOS directions for planets in the Solar System.

planet	$\|\boldsymbol{v}\|$ (km/s)	$\|\boldsymbol{\beta}\|$	$\|\boldsymbol{\beta}\|^2$	$\Delta\theta$ (arcsec)	$\Delta\theta^{LOST}$ (mas)
Mercury	47.87	1.5968×10^{-4}	2.5497×10^{-8}	32.9358	5.2591
Venus	35.02	1.1681×10^{-4}	1.3646×10^{-8}	24.0946	2.8146
Earth	29.78	9.9335×10^{-5}	9.8675×10^{-9}	20.4894	2.0353
Mars	24.08	$8.0322e \times 10^{-5}$	6.4517×10^{-9}	16.5677	1.3308
Jupiter	13.1	4.3697×10^{-5}	1.9007×10^{-9}	9.0131	0.3939
Saturn	9.69	3.2322×10^{-5}	1.0447×10^{-9}	6.6670	0.2155
Uranus	6.81	2.2716×10^{-5}	5.1600×10^{-10}	4.6855	0.1064
Neptune	5.43	1.8113×10^{-5}	3.2806×10^{-10}	3.7360	0.0676

We see from this that estimating the light time-of-flight with the LOST range equation allows to reduce the angular error by a factor about $\|\boldsymbol{\beta}\|$. At the velocities of the planets, this means four to five orders of magnitude lower than the non-corrected angular error (see Table 3). The errors for the corrected LOS are on the order of milliarc-seconds or lower, which is well below the noise floor of current OPNAV sensors. The advantage of using the LOST range equation for the light time-of-flight compensation is that it can be incorporated directly into the LOST solution at almost no additional cost. Thus we can achieve light time-of-flight correction without iteration.

Clearly, with an estimate of Δt_i, the position of the object when it emitted the light ($\boldsymbol{p}_i$) can be fetched from the ephemerides catalog. However another query is often not necessary and we may use $\boldsymbol{p}_i'$ and $\boldsymbol{v}_i' = \boldsymbol{v}_i$ from the observation time. To see this, observe that we may write to an excellent approximation

$$
\begin{aligned}
\boldsymbol{p}_i &= \boldsymbol{p}_i' - \Delta\hat{t}\boldsymbol{v}_i \\
&= \boldsymbol{p}_i' - (\hat{\rho}_i/c)\boldsymbol{v}_i \\
&= \boldsymbol{p}_i' - \hat{\rho}_i\boldsymbol{\beta}_i
\end{aligned}
\tag{70}
$$

and, after substituting from Eq. (13)

$$
\boldsymbol{p}_i = \boldsymbol{p}_i' - \frac{\|\bar{\boldsymbol{x}}_i\|}{\sigma_{x_i} q_i}\boldsymbol{\beta}_i
\tag{71}
$$

The right-hand term in the LOST solution can then be written as

$$
\begin{aligned}
q_i \boldsymbol{S}\left[\bar{\boldsymbol{x}}_i\times\right]\boldsymbol{T}_{C_i}^I \boldsymbol{p}_{I_1}^- &= q_i \boldsymbol{S}\left[\bar{\boldsymbol{x}}_i\times\right]\boldsymbol{T}_{C_i}^I \left(\boldsymbol{p}_i - \frac{\|\bar{\boldsymbol{x}}_i\|}{\sigma_{x_i} q_i}\boldsymbol{\beta}_i\right) \\
&= \boldsymbol{S}\left[\bar{\boldsymbol{x}}_i\times\right]\boldsymbol{T}_{C_i}^I \left(q_i \boldsymbol{p}_i - \frac{\|\bar{\boldsymbol{x}}_i\|}{\sigma_{x_i}}\boldsymbol{\beta}_i\right) \\
&= \boldsymbol{S}\left[\bar{\boldsymbol{x}}_i\times\right]\boldsymbol{T}_{C_i}^I \left(q_i \boldsymbol{p}_i - \boldsymbol{m}_i\right)
\end{aligned}
\tag{72}
$$

where

$$
\boldsymbol{m}_i = \frac{\|\bar{\boldsymbol{x}}_i\|}{\sigma_{x_i}}\boldsymbol{\beta}_i
\tag{73}
$$

and can be computed directly from information we already have. Thus, we modify Eq. 14 to conveniently account for the time of light

$$
\begin{bmatrix}
q_1 \boldsymbol{S}\left[\bar{\boldsymbol{x}}_1\times\right]\boldsymbol{T}_{C_1}^I \\
q_2 \boldsymbol{S}\left[\bar{\boldsymbol{x}}_2\times\right]\boldsymbol{T}_{C_2}^I \\
\vdots \\
q_n \boldsymbol{S}\left[\bar{\boldsymbol{x}}_n\times\right]\boldsymbol{T}_{C_n}^I
\end{bmatrix}
\boldsymbol{r}_I =
\begin{bmatrix}
\boldsymbol{S}\left[\bar{\boldsymbol{x}}_1\times\right]\boldsymbol{T}_{C_1}^I (q_1\boldsymbol{p}_{I_1} - \boldsymbol{m}_{I_1}) \\
\boldsymbol{S}\left[\bar{\boldsymbol{x}}_2\times\right]\boldsymbol{T}_{C_2}^I (q_2\boldsymbol{p}_{I_2} - \boldsymbol{m}_{I_2}) \\
\vdots \\
\boldsymbol{S}\left[\bar{\boldsymbol{x}}_n\times\right]\boldsymbol{T}_{C_n}^I (q_n\boldsymbol{p}_{I_n} - \boldsymbol{m}_{I_n})
\end{bmatrix}
\tag{74}
$$

We see that this allows for statistically optimal triangulation that automatically corrects for light time-of-flight at no meaningful increase in computational expense.

Conclusion. This work reviews the newly developed LOST algorithm for optimal triangulation and highlights three important real-world effects for celestial navigation. Firstly, the effects of the planetary ephemeris (position) uncertainties were considered and found to be negligible everywhere except in the close vicinity of planets. The LOST algorithm proves useful to correct the covariance. Secondly, light aberration is an important effect to consider. If stars within the OPNAV image are used to compute the attitude it may not be necessary to explicitly correct for light aberration, though we provide the equations to do so analytically if needed. Thirdly, the light time-of-flight affects both range and direction. The change in LOS direction due to the time of light travel is not negligible, but can be conveniently accounted for within the LOST framework. In conclusion, LOST not only gives a non-iterative and statistically optimal solution to the triangulation problem for many measurements, but it also allows us to elegantly correct the effects encountered in celestial navigation.

References.

[1] R. R. Karimi and D. Mortari, "Interplanetary Autonomous Navigation Using Visible Planets," *Journal of Guidance, Control, and Dynamics*, vol. 38, no. 6, pp. 1151–1156, 2015, 10.2514/1.G000575.

[2] S. B. Broschart, N. Bradley, and S. Bhaskaran, "Kinematic Approximation of Position Accuracy Achieved Using Optical Observations of Distant Asteroids," *Journal of Spacecraft and Rockets*, vol. 56, no. 5, pp. 1383–1392, 2019, 10.2514/1.A34354.

[3] N. Bradley, Z. Olikara, S. Bhaskaran, and B. Young, "Cislunar Navigation Accuracy Using Optical Observations of Natural and Artificial Targets," *Journal of Spacecraft and Rockets*, vol. 57, no. 4, pp. 777–792, 2020, 10.2514/1.A34694.

[4] V. Franzese and F. Topputo, "Deep-space optical navigation exploiting multiple beacons," *The Journal of the Astronautical Sciences*, vol. 69, pp. 368–384, 2022, 10.1007/s40295-022-00303-5.

[5] S. Henry and J. A. Christian, "Absolute triangulation algorithms for space exploration," *Journal of Guidance, Control, and Dynamics*, vol. 0, no. 0, pp. 1–26, 0, 10.2514/1.G006989.

[6] J. A. Christian, "A Tutorial on Horizon-Based Optical Navigation and Attitude Determination with Space Imaging Systems," *IEEE Access*, pp. 19,819–19,853, 2021, 10.1109/ACCESS.2021.3051914.

[7] R. I. Hartley and A. Zisserman, *Multiple View Geometry in Computer Vision*, 2nd ed. Cambridge University Press, 2004.

[8] Y. I. Abdel-Aziz and H. M. Karara, "Direct linear transformation from comparator coordinates into object space coordinates in close-range photogrammetry," *Photogrammetric Engineering & Remote Sensing*, vol. 81, no. 2, pp. 103–107, 2015, 10.14358/PERS.81.2.103.

[9] R. I. Hartley and P. Sturm, "Triangulation," *Computer Vision and Image Understanding*, vol. 68, no. 2, pp. 146–157, 1997, 10.1006/cviu.1997.0547.

[10] M. N. Armstrong, "Self-calibration from image sequences," Ph.D. dissertation, University of Oxford, 1996.

[11] P. F. Sturm, "Vision 3d non calibrée: Contributions à la reconstruction projective et Étude des mouvements critiques pour l'auti-calibrage," Ph.D. dissertation, Institut National Polytechnique de Grenoble, 1997.

[12] H. Stewenius, F. Schaffalitzky, and D. Nister, "How hard is 3-view triangulation really?" in *Tenth IEEE International Conference on Computer Vision (ICCV'05) Volume 1*, vol. 1, 2005, pp. 686–693 Vol. 1, 10.1109/ICCV.2005.115.

[13] D. P. Lubey, S. Bhaskaran, N. Bradley, and Z. Olikara, "Ice giant exploration via autonomous optical navigation," in *AAS/AIAA Astrodynamics Specialist Conference*, no. AAS 20-673, 2020.

[14] W. Folkner, "Uncertainties in the jpl planetary ephemeris," in *Proceedings of the Journées*, 2010, p. 43.

[15] J. Bradley, "Iv. a letter from the reverend mr. james bradley savilian professor of astronomy at oxford, and f. r. s. to dr. edmond halley astronom. reg. & c. giving an account of a new discovered motion of the fix'd stars," *Philosophical Transactions, The Royal Society*, vol. 34, no. 406, pp. 637–661, 1728, 10.1098/rstl.1727.0064.

[16] A. Einstein, "Zur elektrodynamik bewegter körper," *Annalen der physik*, vol. 322, no. 10, pp. 891–921, 1905, 10.1002/andp.19053221004.

[17] J. A. Christian, "Starnav: Autonomous optical navigation of a spacecraft by the relativistic perturbation of starlight," *Sensors*, vol. 19, p. 4064, 2019, 10.3390/s19194064.

[18] C. O. Hines, "Planetary Aberration," *Nature*, vol. 163, p. 249, 1949, 10.1038/163249a0.

[19] G. H. Kaplan, "High-Precision Algorithms for Astrometry: A Comparison of Two Approaches," *The Astronomical Journal*, vol. 115, pp. 361–372, 1998, 10.1086/300189.

[20] M. D. Shuster, "Stellar Aberration and Parallax: A Tutorial," *The Journal of the Astronautical Sciences*, vol. 51, no. 4, pp. 477–494, Dec. 2003, 10.1007/BF03546295.

[21] F. Markley and J. Crassidis, *Fundamentals of spacecraft attitude determination and control.* New York, NY: Springer, 2014. 10.1007/978-1-4939-0802-8.

[22] G. Wahba, "A least square estimate of satellite attitude," *SIAM Review*, vol. 7, no. 3, p. 409, 1965, 10.1137/1007077.